

# Efficacy of 2,4-Di-*tert*-butylphenol in Reducing *Ralstonia solanacearum* Virulence: Insights into the Underlying Mechanisms

Le Yang,<sup>⊥</sup> Rongbo Wang,<sup>⊥</sup> Wei Lin, Benjing Li, Ting Jin, Qiyong Weng, Meixiang Zhang, and Peiqing Liu\*



Cite This: *ACS Omega* 2024, 9, 4647–4655



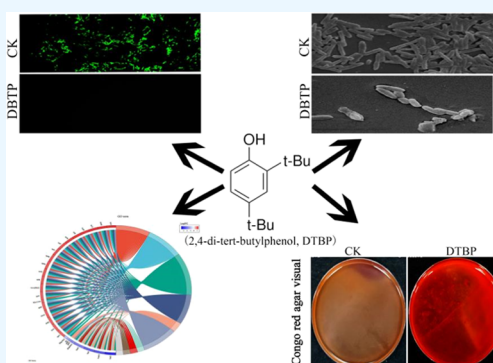
Read Online

ACCESS |

Metrics & More

Article Recommendations

**ABSTRACT:** *Ralstonia solanacearum* can induce severe wilt disease in vital crops. Therefore, there is an urgent need to develop novel antifungal solutions. The natural compound 2,4-di-*tert*-butylphenol (2,4-DTBP) exhibits diverse physiological activities and affects soil function. However, its specific impact on the *R. solanacearum* remains unclear. Here, we investigated the antimicrobial potential of 2,4-DTBP. The results demonstrated that 2,4-DTBP effectively inhibited its growth and altered morphology. In addition, it substantially impeded biofilm formation, motility, and exopolysaccharide secretion. Transcriptomic analysis revealed that 2,4-DTBP inhibited energy production and membrane transport. Additionally, 2,4-DTBP hindered the growth by interfering with the membrane permeability, reactive oxygen species (ROS) production, and electrolyte leakage. Concomitantly, this led to a significant reduction in pathogenicity, as evidenced by the biomass of *R. solanacearum* in the invaded roots. Overall, our data strongly support the potential utility of 2,4-DTBP as a



a potent antibacterial agent capable of effectively preventing the onset of bacterial wilt caused by *R. solanacearum*.

## INTRODUCTION

Bacterial wilt, a pervasive and destructive plant disease, inflicts annual damage of approximately 1 billion US dollars. It is caused by the notorious *Ralstonia solanacearum* species complex.<sup>1–3</sup> *R. solanacearum*, a soil-borne Gram-negative bacterium, demonstrates strong pathogenicity across a spectrum of more than 250 plant species, including potatoes, tomatoes, tobacco, and chili.<sup>4,5</sup> The initial invasion occurs via secondary root emerging points, wounds, or root tips, spreading to aerial parts and resulting in severe plant wilting. The pathogen colonizes the cortex before rapidly advancing to the xylem, where cultured cells grow extensively and yield large amounts of EPS, leading to pronounced vascular obstruction.<sup>6</sup> Data from several studies have indicated that this EPS helped *R. solanacearum* disrupt water and nutrient transportation in host plants.<sup>7</sup> Although chemical control measures have demonstrated efficacy, they are not cost-effective and can lead to substantial environmental pollution, posing risks to consumable crop products.<sup>8</sup> With *R. solanacearum* in growing soil, even outside host plants, it can be challenging to regulate *R. solanacearum* by adopting conventional agricultural approaches, such as crop rotation and resistant cultivars.<sup>9,10</sup> Hence, the development of alternative agents for effective bacterial wilt management has attracted substantial interest as a sustainable and safe solution.

A growing body of evidence substantiates the antibacterial attributes inherent in phenolic acid, a compound that is typically encountered as a ubiquitous plant secondary metabolite within the rhizosphere.<sup>11</sup> Phenolic acids are known for their robust antioxidant activities and for inactivating and stabilizing free radicals in plants.<sup>12</sup> Notably, 2,4-DTBP, a phenolic acid identified in the root exudates of various plants, potently inhibits weed growth.<sup>13</sup> Additionally, 2,4-DTBP is a natural component of medicinal plants such as *Gynura cusimbua* and *Heliotropium indicum*.<sup>14</sup> Research has indicated that 2,4-DTBP can significantly affect enzyme activities in soil, modulating soil microbial diversity.<sup>15</sup> In cucumber cultivation, 2,4-DTBP initially stimulated an increase in root microbes, followed by a significant decline as 2,4-DTBP concentration increased.<sup>16</sup> EPS are pivotal in bacterial biofilm formation, with 2,4-DTBP inhibiting EPS secretion, thereby facilitating biofilm disruption and eventual eradication.<sup>17</sup> Recently, 2,4-DTBP has been employed to reduce biofilm formation by *Pseudomonas aeruginosa*.<sup>18</sup> In

**Received:** October 9, 2023

**Revised:** December 23, 2023

**Accepted:** December 28, 2023

**Published:** January 16, 2024



addition, 2,4-DTBP opens new avenues for innovative antifungal strategies targeting *Mycobacterium tuberculosis* and *Candida albicans*.<sup>19</sup>

Recent studies have highlighted the capacity of 2,4-DTBP in the rhizosphere of weeds to rapidly induce notable oxidative stress by triggering numerous reactive oxygen species (ROS), resulting in pronounced lipid peroxidation and membrane damage.<sup>20</sup> Generally, lipid peroxidation is induced by superoxide radicals, hydrogen peroxide, and singlet oxygen. ROS can target lipids containing characteristic carbon–carbon double bonds.<sup>21</sup> Studies have reported correlations among energy metabolism, carbohydrate pathways, and lipid metabolism. Lipid peroxidation is an indicator of ROS-induced oxidative stress, and membrane integrity can be altered.<sup>22</sup> Previously, the permeability and integrity of the membrane are the key regulatory factors for various cellular functions (e.g., electric conductivity and pathogenicity). The impairment in plasma membrane followed by leakage of cytoplasmic contents (e.g., nucleic acids and proteins), which ultimately leads to the destruction of cell structure and suppresses the expression of pathogenicity-related genes, leads to reduced infection activity.<sup>20</sup> Although the precise potential of 2,4-DTBP against bacterial biofilms remains unexplored, the exploration of ROS and membrane damage has been suggested as a valuable avenue for predicting its effects on *R. solanacearum*.

The objective of this study was to analyze the function of 2,4-DTBP in reducing *R. solanacearum* virulence and its underlying mechanisms. Specifically, we analyzed three key questions. First, does 2,4-DTBP inhibit growth and morphology? Second, does 2,4-DTBP impede virulence, motility, and biofilm formation? Third, are the potential physiological and biochemical mechanisms involved in 2,4-DTBP inhibition of *R. solanacearum*? Based on the results of this study, we hypothesized that 2,4-DTBP effectively reduced the growth and pathogenicity of *R. solanacearum*. Our endeavor centers on exploring ecofriendly methods to mitigate bacterial wilt.

## MATERIALS AND METHODS

**Strains and Culture Conditions.** The *R. solanacearum* strain (Standard strain GMI 1000) was used in this study. *R. solanacearum* was routinely grown on a nutrient agar (NA) medium (0.5 g L<sup>-1</sup> yeast extract, 5 g L<sup>-1</sup> peptone, 10 g L<sup>-1</sup> glucose, 3 g L<sup>-1</sup> beef extract, and 20 g L<sup>-1</sup> agar) at 30 °C. NA medium was prepared in an autoclave (MLS-3750, SANYO) at 121 °C and 15 Psi (1.05 kg cm<sup>-2</sup>) for 15 min and then used for growth. 2,4-DTBP was purchased from Sigma-Aldrich. Bacterial growth was determined by measuring optical density at a wavelength of 600 nm.

**Influence of 2,4-DTBP on the Growth of *R. solanacearum*.** 2,4-DTBP was obtained from Sigma-Aldrich Co., Ltd. (Shanghai, China), and a stock solution of 10 mM was prepared by dilution in dimethyl sulfoxide (DMSO). A 2  $\mu$ L aliquot of freshly cultured *R. solanacearum* (1  $\times$  10<sup>5</sup> CFU/mL) was directly spread onto nutrient agar plates containing 2,4-DTBP at concentrations of 0.0, 0.1, 0.5, 1.0, and 2.0 mM. Bacterial growth was determined by measuring the optical density at a wavelength of 600 nm. *R. solanacearum* treated with DMSO was used as a control. After 36–48 h of incubation at 28 °C, the viable colonies were enumerated. The inhibitory effect of 2,4-DTBP on cell viability was assessed by using colony-forming unit (CFU) counts. Cell viability (%) was calculated using the formula cell viability (%) =  $V'/V \times 100\%$ , where  $V'$  represents the CFUs on 2,4-DTBP

concentrations (0.1, 0.5, 1.0, and 2.0 mM) and  $V$  represents colonies on the control. For growth curve analysis, 100  $\mu$ L of freshly cultured *R. solanacearum* (1  $\times$  10<sup>9</sup> CFU/mL) was transferred to an NB medium with 0.5 mM 2,4-DTBP. Incubation at 28 °C spanned over 36 h, with continuous agitation on a shaking table at 180 rpm. OD<sub>600</sub> was measured at 4 h intervals, and visual documentation was captured using a Sony  $\alpha$ 7 camera.

**Influence of 2,4-DTBP on the Morphology of *R. solanacearum*.** SEM was employed to investigate alterations in morphology by 0.5 mM 2,4-DTBP. Freshly cultured *R. solanacearum* was diluted to 1  $\times$  10<sup>9</sup> CFU/mL in NB medium and incubated at 28 °C with agitation at 180 rpm on a shaker. After 16 h, the *R. solanacearum* cells were centrifuged at 7000 rpm for 5–8 min and the supernatant was removed. Subsequently, cells were subjected to triple washing with phosphate buffer (0.1 mol/L, pH 7.0) and fixed using 2.5% glutaraldehyde at 4 °C. The SEM analysis was conducted following the procedures outlined by Pelyuntha et al.<sup>18</sup>

**Effect of 2,4-DTBP on Biofilm Formation of *R. solanacearum*.** Cultured *R. solanacearum* (1  $\times$  10<sup>9</sup> CFU/mL) treated with 0.5 mM 2,4-DTBP was introduced in 100  $\mu$ L into individual wells of a 96-well microtiter plate. The plates were subsequently wrapped with a cling wrap and incubated in the dark at 28 °C for 16 h. Subsequently, the liquid medium was discarded, and the wells were rinsed three times with distilled water. The plates were then stained with 0.1% crystal violet for 25–30 min, followed by washing with distilled water. Crystal violet was removed from the biofilm using 200  $\mu$ L of 95% ethanol. The biofilm density was measured by using a microplate reader at 490 nm.

We used a visual qualitative assay on Congo red agar to investigate the inhibition of biofilm formation. Specifically, 0.08% Congo red was introduced into the NA plates along with 0.5 mM 2,4-DTBP. Freshly cultured *R. solanacearum* was streaked onto plates and incubated at 28 °C for 36–48 h. The presence of dry crystalline black colonies on Congo red plates also confirmed EPS production by *R. solanacearum*.

**Defection of 2,4-DTBP on the EPS.** With 0.5 mM 2,4-DTBP, the supernatant of freshly cultured *R. solanacearum* cells was subjected to precipitation by using three volumes of chilled 100% ethanol. The mixture was incubated for 24–36 h at 4 °C. The resulting cell precipitate was centrifugated at 10 000–12 000 rpm for 15 min, followed by dissolution in freshwater. Additionally, EPS content was quantified using the phenol-sulfuric acid method. Subsequently, H<sub>2</sub>SO<sub>4</sub> was added to 1 mL of the suspension, and the resulting mixture was quantified spectrophotometrically at 490 nm.

**Impact of 2,4-DTBP on the Motility of *R. solanacearum*.** CPG plates were used for the motility analysis. A 2  $\mu$ L droplet of freshly cultured *R. solanacearum* was deposited into Milli-Q (OD<sub>600</sub> = 0.1) in the middle of the plate. Incubation was performed at 28 °C for 60–72 h, during which the swimming behaviors were meticulously recorded.

**Transcriptome Analysis.** RNA was extracted from freshly cultured *R. solanacearum* cells treated with 0.5 mM 2,4-DTBP, along with evaluation of its concentration and quality. A total of 3–5  $\mu$ g of RNA was obtained using an RNA Library Prep Kit, followed by cDNA synthesis. The samples were sequenced, yielding reads of approximately 150–200 bp. Quality assessment of the raw RNA-Seq data was conducted using FastQC. The recently obtained NZ\_CP016914.1 genome from GeneBank was adopted as the reference, and the

alignment of the reads to reference sequences was conducted using Bowtie2-2.2.3. The read count per gene was determined using HTSeq v0.6.1, followed by FPKM calculation. Identification of DEGs was executed through the DESeq R package (1.18.0). GO analysis was conducted using the R56. KEGG pathway analysis was then performed, and pathways with a corrected  $p < 0.05$  were considered significantly enriched among DEGs.

**Cell Membrane Integrity Analysis.** *R. solanacearum* was cultivated with 0.5 mM 2,4-DTBP for 16 h at 28 °C. Following the removal of the supernatant, fresh NB medium with 0.5 mM 2,4-DTBP was added and incubated for an additional 4 h without agitation. Bacteria were initially washed with Milli-Q water and subsequently stained with SYTO 9 and PI components. The stained bacterial samples were then incubated in the dark for 15–20 min and observed under a microscope.

**Influence of 2,4-DTBP on the Electric Conductivity.** Freshly cultured *R. solanacearum* treated with 0.5 mM 2,4-DTBP underwent centrifugation and subsequent triple washes. Subsequently, the bacteria were resuspended in 0.1 M phosphate buffer (pH = 7.4) to a concentration of  $10^8$  CFU/mL. Electric conductivity measurements were then recorded at 10 min intervals over a duration of 30 min.

**Impact of 2,4-DTBP on the ROS.** The cells were exposed to 0.5 mM 2,4-DTBP for 4 h. Subsequently, the cells were washed three times with sterilized water. Subsequently, 10  $\mu$ M DCFH-DA was added to the cells, which were then incubated in the darkness at 28–30 °C for 30–40 min. The resulting green fluorescence was assessed after washing with sterilized water.

**Impact of 2,4-DTBP on the Colonization.** Tomato seedling roots were immersed in 0.5 mM 2,4-DTBP for 30–40 min, followed by cultivation in MS medium with 1 mL of  $1 \times 10^9$  CFU/mL *R. solanacearum*. Adherence of cells to the root surface was evaluated over a span of 1–7 d at 28 °C. Subsequently, the seedling roots were immersed in 75% ethanol for 10 min, followed by washing thrice with sterile water. One gram amount of seedling roots was pulverized using a mortar and pestle, followed by homogenization in 5 mL of sterile water. A 1 mL suspension was deposited onto NA plates, and colony enumeration was performed.

**Quantitative RT-PCR Analysis.** Total RNA was extracted according to the manufacturer's guidelines. DNase treatment was performed to eliminate any potential genomic DNA. One microgram of RNA was used to obtain cDNA, and qPCR was performed as previously described. The glyceraldehyde 3-phosphate dehydrogenase (*GAPDH*) gene of tomato was used as the internal reference,<sup>23</sup> and the specific amplification of *R. solanacearum* was carried out using the *RSF* gene (Table 1). Custom primers for the evaluated pathogenic genes were designed by using the Primer5 software.

**Statistical Analysis.** All assays were conducted with a minimum of three replicates. The collected data were subjected to a one-way analysis of variance (ANOVA) in the SPSS 19.0 software (IBM Corp., Armonk, NY). Subsequently, the Tukey test was conducted to identify significant differences among different treatments. The difference in means was determined using the Tukey test with a  $P$  value of  $<0.05$ .

## RESULTS

**Effect of 2,4-DTBP on the Growth and Morphological Changes.** In this study, various concentrations of 2,4-DTBP

**Table 1. Primer Sequences**

gene	primer sequence (5'–3')
<i>RSF</i>	forward: GTGCCTGCCTCCAAAACGACT reverse: GACGCCACCCGCATCCCTC
<i>RipAB</i>	forward: GCACGATGGTCTCGCTCAAGTC reverse: TCTTCTTGCCGCTTCGGTTTC
<i>RipA1</i>	forward: TCGACTGACCACGACACTGACC reverse: ATGCCTTCTCGCGCTGTCT
<i>RipE1</i>	forward: CAGTTCGGCGGCTATCTGATGG reverse: GCGGGGTTTGCAGCAGTGT
<i>GAPDH</i>	forward: ACCACAAATTGCCTTGCTCCCTTG reverse: ATCAACGGTCTTCTGAGTGGCTGT

(0.1, 0.5, 1.0, and 2.0 mM) were investigated for their potent antibacterial activity (Figure 1). Employing a plate counting method, cell viability assessment demonstrated 76, 58, 53, and 35% viabilities at concentrations of 0.1, 0.5, 1.0, and 2.0 mM, respectively (Figure 1B). Though there was a statistically significant association between the concentrations of 0.5 and 1.0 mM, we anticipate that lower concentrations will be more suitable for field use. Additionally, we chose 0.5 mM for determining its inhibitory effect. Furthermore, growth curve calculation indicated a substantial reduction in growth at 16 h for 0.5 mM 2,4-DTBP (Figure 1C). Interestingly, 0.5 mM 2,4-DTBP also contributed to growth inhibition, thereby affecting the colony shape of *R. solanacearum*. A decrease in the level of red colony formation was observed (Figure 1D). Morphological changes due to the 0.5 mM 2,4-DTBP treatment were tracked using SEM after 16 h. Untreated freshly cultured cells exhibited long rod shapes, complete membrane structures, and smooth textures (Figure 1D). Conversely, cells treated with 0.5 mM 2,4-DTBP significantly inhibited the surface structures and morphologies. At 0.5 mM 2,4-DTBP, a reduction in cell length and significantly decreased cell diameters was evident (Figure 1D).

**Impact of 2,4-DTBP on the Biofilm Formation and Motility.** After a 16 h period, the impact of 0.5 mM 2,4-DTBP on biofilm formation was evaluated. The findings indicated an 80% reduction in biofilm formation, owing to the inhibitory effects of 0.5 mM 2,4-DTBP (Figure 2A). Furthermore, the application of Congo red agar indicated an absence of black colonies upon treatment with 0.5, 1.0, and 2.0 mM 2,4-DTBP (Figure 2C), suggesting an inability to robustly produce biofilm production. In addition, the secretion of *R. solanacearum*'s EPS was significantly impeded by 0.5 mM 2,4-DTBP, resulting in an 81.5% reduction (Figure 2B). After 48 h, the impact of 0.5 mM 2,4-DTBP was found to reduce swimming activity (Figure 2D). This reduction in the swimming ability was accompanied by a significant reduction in the migratory zone diameter (Figure 2E).

**Impact of 2,4-DTBP on the Transcriptome.** The results presented in Figure 3 highlight significant changes in pathways upon treatment with 0.5 mM 2,4-DTBP based on our comprehensive analyses of volcano plots, GO, chordal graphs, and KEGG annotations. In addition, 472 genes exhibited differential expression, comprising 113 upregulated and 359 downregulated genes (Figure 3A). GO analysis revealed a diverse distribution of DEGs across biological processes, cellular components, and molecular functions. Enriched biological processes included binding, transporter activity, structural molecular activity, ATP-dependent activity, and transcriptional regulation (Figure 3B). Chordal graph analysis

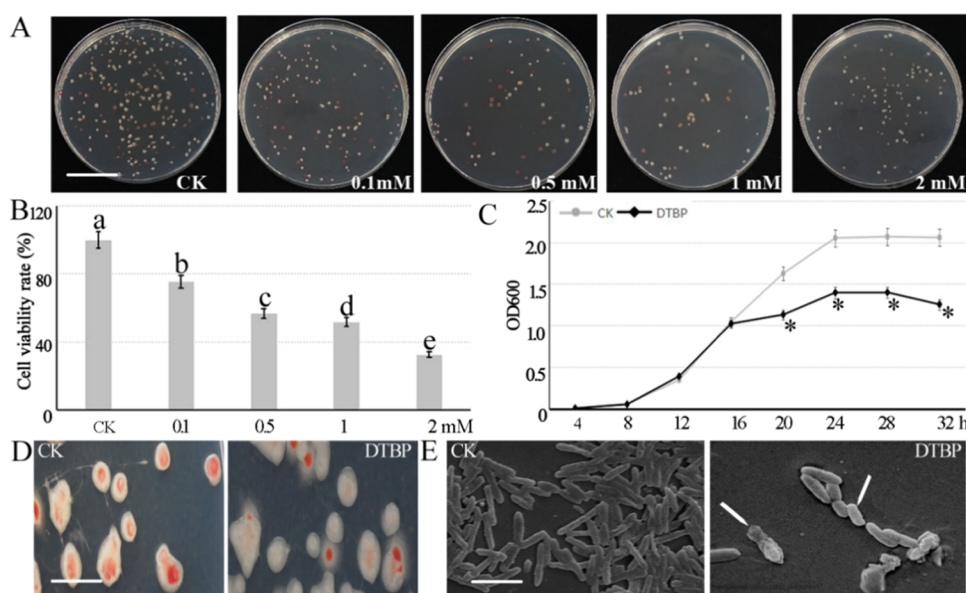


**Figure 1.** Antibacterial activity of 2,4-DTBP against *R. solanacearum*. (A) Growth on NA plates after 36–48 h of culture. (B) Impact of 2,4-DTBP on the cell viability rate. Means followed by the same letter are not significantly different ( $p < 0.05$ ) among treatments. (C) Growth curves inhibited by 2,4-DTBP. The symbol (\*) indicates a significant difference between treatment and control at  $P < 0.05$  for each time. (D) Microscopic observations of the decreased red colony formation in *R. solanacearum*. (E) SEM images of cells affected by 2,4-DTBP (scale bar = 2  $\mu\text{m}$ ). Assays were repeated three times.  $n = 4$  for each assay. *R. solanacearum* treated with DMSO was used as a control.

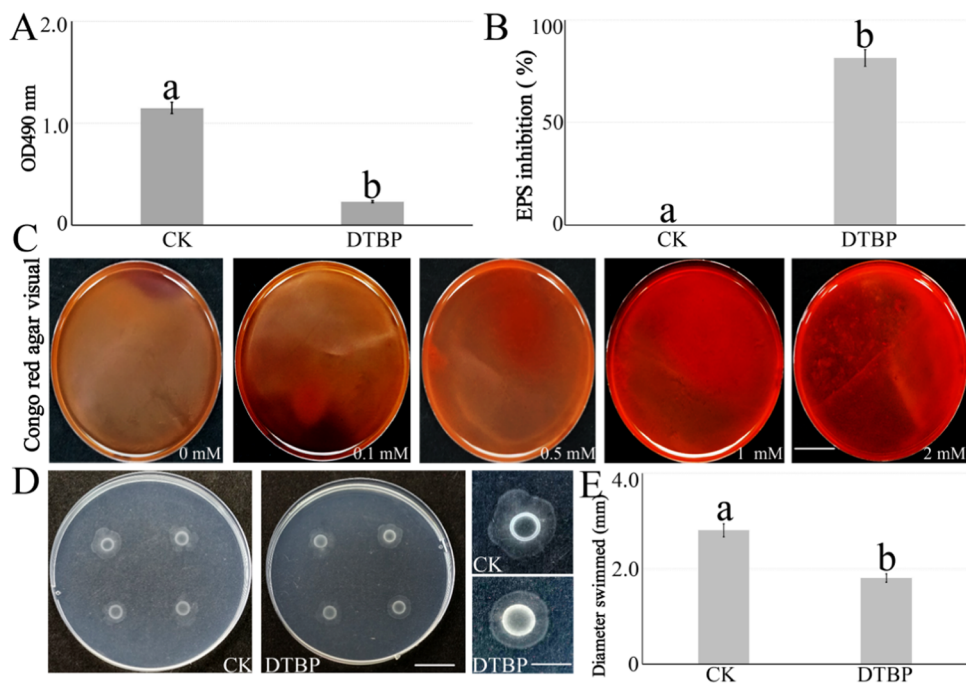


**Figure 2.** Inhibition of *R. solanacearum* biofilm, EPS, and swimming by 2,4-DTBP. (A) Inhibition of 0.5 mM 2,4-DTBP on biofilm formation. Means followed by the same letter are not significantly different ( $p < 0.05$ ) among treatments. (B) Effects of various concentrations of 2,4-DTBP on EPS. Means followed by the same letter are not significantly different ( $p < 0.05$ ) among treatments. (C) Visual qualitative assay for the inhibition of biofilm formation on Congo red agar (scale bar = 25 mm). (D) Inhibition of the *R. solanacearum* swimming motility (scale bar = 25 mm). (E) Inhibition of *R. solanacearum* swarming ability. Means followed by the same letter are not significantly different ( $p < 0.05$ ) among treatments. Assays were repeated three times.  $n = 4$  for each assay. *R. solanacearum* treated with DMSO was used as a control.

highlighted the regulatory impact of 0.5 mM 2,4-DTBP on KEGG pathways including peptide biosynthetic processes, translation, peptide metabolic processes, and cellular amide metabolic processes (Figure 3C). Most DEGs were associated with energy metabolism, carbohydrate metabolism, xenobiotic biodegradation, biosynthesis of secondary metabolites, nucleo-

tide metabolism, glycan biosynthesis, terpenoids, polyketides, and lipid metabolism (Figure 3D). Notably, pathways related to carbon, energy, and lipid metabolism were directly related to the pathogenic process.

#### Influence of 2,4-DTBP on the Membrane Damage.

Iodide (PI) and SYTO 9 staining were used to analyze the

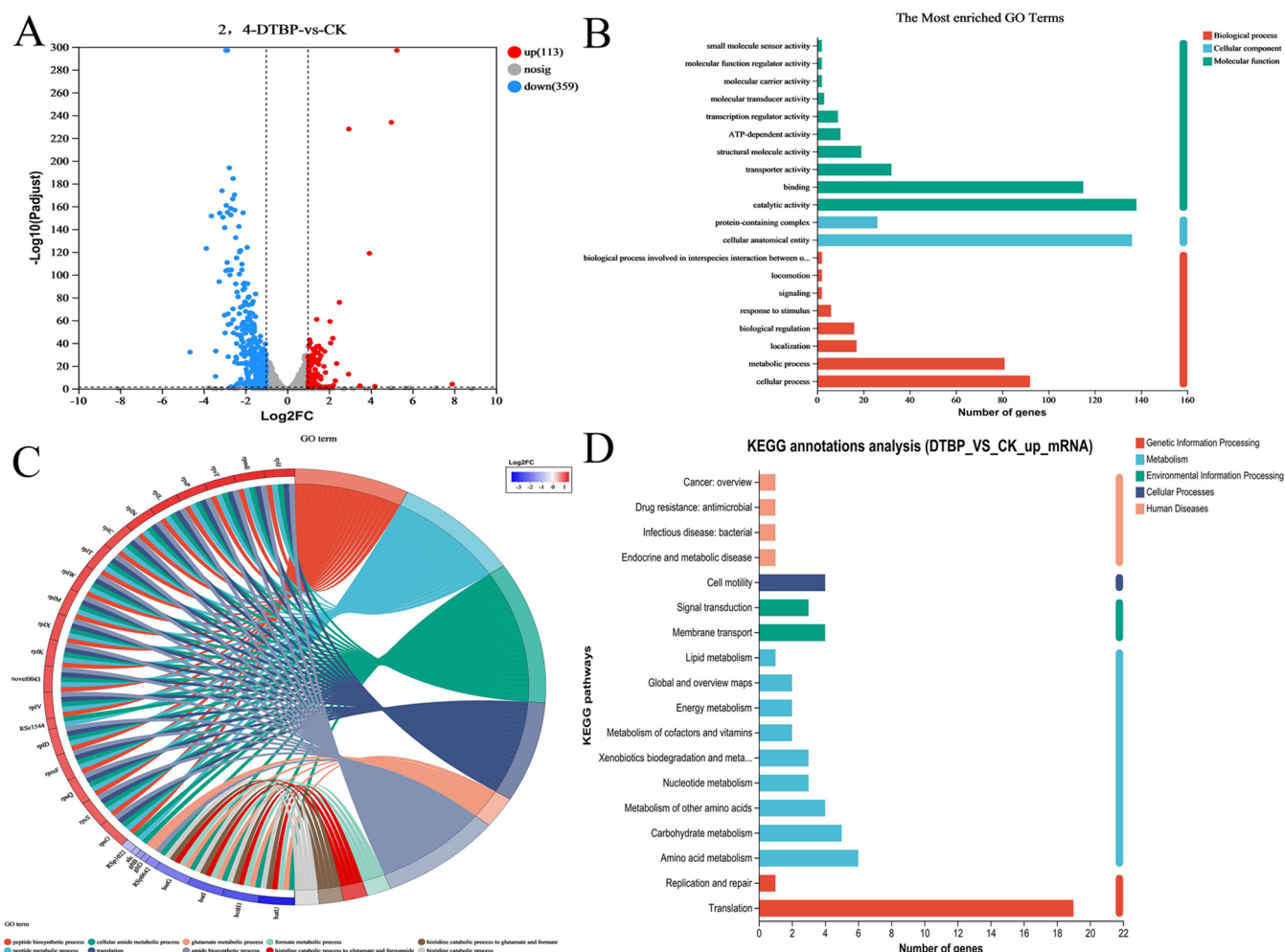


**Figure 3.** Transcriptomic changes induced by 2,4-DTBP. (A) Volcano plot of genes affected by 2,4-DTBP. (B) Biological function enrichment analysis of DEGs using GO. (C) Chordal graph analysis. (D) KEGG analysis of DEGs. CK represents the control, while 2,4-DTBP represents *R. solanacearum* treated with 0.5 mM 2,4-DTBP.

differences between permeabilized and total cells attributed to 0.5 mM 2,4-DTBP. As depicted in Figure 4A, cells treated with 0.5 mM 2,4-DTBP demonstrated red staining, indicative of dead or dying cells with compromised membranes, whereas cells with intact membranes (e.g., the control) exhibited green staining. This observation indicated that 0.5 mM 2,4-DTBP resulted in a cell membrane disruption. ROS levels were assessed using DCFH-DA staining (Figure 4B). The absence of green fluorescence in the 0.5 mM 2,4-DTBP-treated cells contrasted with the green fluorescence observed in the control cells. Moreover, the application of 0.5 mM 2,4-DTBP resulted in a 25% reduction in the electrical conductivity after 30 min of treatment (Figure 4C).

**Influence of 2,4-DTBP on the Pathogenicity.** To explore the impact of 2,4-DTBP on virulence, we compared the relative expression levels of the pathogenicity-related genes *RipA1*, *RipE1*, and *RipAB*. As shown in Figure 5, the expression of *RipA1* and *RipE1* was notably inhibited at 3 hpi (Figure 5B,5C), whereas *RipAB* expression was hindered at 6 hpi (Figure 5A). Regarding the pathogen biomass in infected tomato plants, a steady increase was observed at 1 day postexposure, peaking at 5 dpi. In contrast, the biomass of *R. solanacearum* was only detectable after 7 dpi in tomato plants treated with 2,4-DTBP, and no *R. solanacearum* DNA content

was detected in either 2,4-DTBP-treated tomato plants or the control (Figure 5D). These results collectively indicated that 0.5 mM 2,4-DTBP effectively inhibited *R. solanacearum* pathogenicity and colonization.

## DISCUSSION

2,4-DTBP is a lipophilic phenolic compound identified in various plants, and previous studies have highlighted its antifungal properties.<sup>24–26</sup> Our present study suggests the distinct inhibitory potential of different concentrations of 2,4-DTBP on *R. solanacearum* growth (Figure 1). This inhibition can be succinctly illustrated by the cell viability, which was 76, 58, 53, and 35% at 0.1, 0.5, 1.0, and 2.0 mM 2,4-DTBP. These results corroborate the findings of previous studies involving *C. albicans*, *M. tuberculosis*, and *Acinetobacter baumannii*, demonstrating the utility of phenolic compounds for sterilization in food and medical applications.<sup>27–29</sup> In addition, we observed alterations in the morphology of *R. solanacearum* cells in response to 2,4-DTBP treatment (Figure 1D). Subsequent SEM analysis further demonstrated that 2,4-DTBP disrupted the cell morphology (Figure 1E). Moreover, the SEM findings indicated a notable reduction in biofilm formation, along with a decreased surface area affected by 2,4-DTBP. Notably, it was

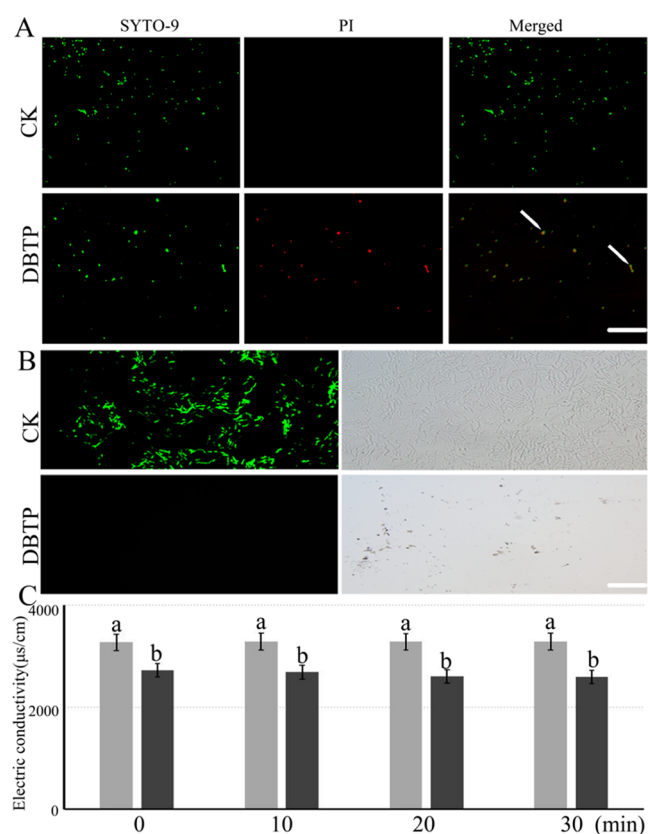


**Figure 4.** Influence of 2,4-DTBP on the membrane damage. (A) Live/dead imaging using PI and SYTO 9 dual stain (scale bar = 20  $\mu\text{m}$ ). CK represents untreated *R. solanacearum*, while 2,4-DTBP represents *R. solanacearum* treated with 0.5 mM 2,4-DTBP. (B) Detection of ROS using DCFH-DA and fluorescence microscopy (scale bar = 10  $\mu\text{m}$ ). CK represents untreated *R. solanacearum*, while 2,4-DTBP represents *R. solanacearum* treated with 0.5 mM 2,4-DTBP. The scale bar is equivalent to 20 mm. (C) Electronic conductivity changes in *R. solanacearum* induced by 0.5 mM 2,4-DTBP. All experiments were performed in triplicate. Values are expressed as mean  $\pm$  SE ( $n = 4$ ). Left represents the control, while right represents treatment with 0.5 mM 2,4-DTBP. Means followed by the same letter are not significantly different ( $p < 0.05$ ) among treatments.

intriguing to observe that 2,4-DTBP has been previously reported to exert an allelopathic effect on weed germination.<sup>30</sup>

Bacteria in biofilms exhibit robust resistance to antibacterial agents, and phenols have been shown to enhance biofilm formation in *Streptococcus mitis*, *Fusobacterium nucleatum*, and *Porphyromonas gingivalis*.<sup>31,32</sup> Surprisingly, our results indicated a notable absence of black colonies in the presence of 0.5, 1, and 2 mM 2,4-DTBP on Congo red agar (Figure 2C), suggesting their ability to inhibit biofilm formation. Previous studies have elucidated the inhibitory effects of phenol, including the disruption of cell membranes.<sup>33</sup> In this study, we observed that 0.5 mM 2,4-DTBP led to an 80% reduction in biofilm formation and an 81.5% inhibition of *R. solanacearum* EPS secretion (Figure 2). This substantial reduction suggests the potential of 2,4-DTBP as an antibiofilm candidate. Recently, phenols, such as betulin in *P. aeruginosa*, have emerged as anti-QS candidates, resulting in the formation of pink colonies.<sup>34</sup> Similarly, in *C. albicans*, 2,4-DTBP inhibited EPS production by approximately 33% in *Streptococcus* sp.,<sup>35</sup> which is in agreement with our findings. In contrast, 2,4-DTBP did not significantly affect the morphology of *Fusarium fujikuroi*.<sup>36,37</sup> Moreover, our investigation demonstrated that 0.5 mM 2,4-DTBP reduced the swimming behavior of *R. solanacearum* in Petri dishes (Figure 2D) and significantly decreased the migratory zone diameter (Figure 2E). The underlying relationships between phenol-induced changes in physiological traits may be partly elucidated using transcriptome analysis.<sup>38</sup> Therefore, we conducted a detailed analysis of the genes and metabolites associated with 2,4-DTBP. Following treatment with 2,4-DTBP, we observed changes in 472 genes, with 113 significantly upregulated and 359 significantly downregulated genes, suggesting the involvement of 2,4-DTBP in antibacterial activity. KEGG pathway analysis showed that energy, carbohydrate, and lipid metabolic pathways were notably affected by 2,4-DTBP (Figure 3). Previous studies have indicated that fungicides commonly target carbon metabolism, energy metabolism, and membrane transport pathways.<sup>39–41</sup>

ROS plays a crucial role as swiftly generated molecules under external stress.<sup>42,43</sup> In this study, we used propidium iodide (PI) and SYTO 9 to analyze both permeabilized and

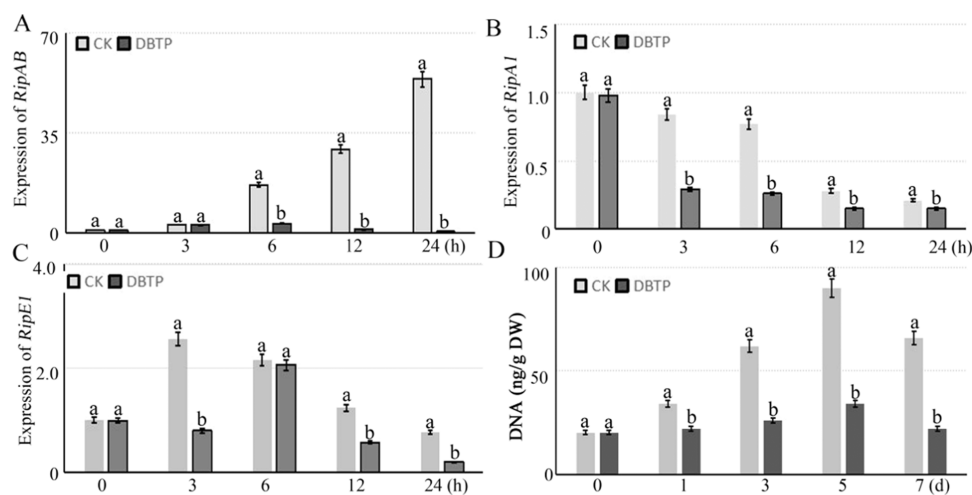


**Figure 5.** Effects of 2,4-DTBP on the pathogenicity. (A) Relative transcript levels of RipAB (A), RipA1, (B), and RipE1 (C). (D) *R. solanacearum* DNA content in *R. solanacearum*-infected seedlings. Experiments were repeated three times. Values are expressed as mean  $\pm$  SE ( $n = 4$ ). Means followed by the same letter are not significantly different ( $p < 0.05$ ) among treatments.

total cells. As depicted in Figure 4, 0.5 mM 2,4-DTBP resulted in substantial damage or deterioration of the cell membranes. Additionally, ROS levels were quantified using DCFH-DA staining. Following a 16 h treatment with 0.5 mM 2,4-DTBP, we observed a complete absence of green fluorescence (Figure 4B). Previous studies have indicated that excessive accumulation of ROS can lead to electrolyte leakage, which can be detected immediately.<sup>44,45</sup> Notably, our findings demonstrated that 0.5 mM 2,4-DTBP resulted in a 25% reduction in electrical conductivity after a 30 min treatment period (Figure 4C). This suggested that prolonged exposure of *R. solanacearum* to 0.5 mM 2,4-DTBP can induce significant ion leakage. Transcriptome analysis has also provided insights into phenol-induced ROS accumulation in *Fusarium oxysporum*, disrupting cell wall integrity and virulence.<sup>46</sup> Bacterial physiological activities, such as virulence and pathogenesis, play pivotal roles in *R. solanacearum* infection.<sup>47,48</sup> Previous studies have reported a strong correlation between the expression of pathogenicity-related genes and colonization.<sup>49,50</sup> Especially, the type III secretion system with its delivered type III effectors is the main virulence determinants of *R. solanacearum*, and more than 100 different type III effectors have been identified.<sup>51</sup> Among them, the cytoplasm and plasma membrane RipA1 can induce cell death with varying intensities on different plants, the nuclear T3E RipAB inhibits the expression of Ca<sup>2+</sup>-related defense genes, and RipE1 can be perceived in planta by intracellular immune-Nod-like receptors (NLRs) and induces the synthesis of salicylic acid and jasmonic acid to trigger immunity.<sup>51</sup> Compared to the control, 0.5 mM 2,4-DTBP notably inhibited the expression of RipAB by 100% (Figure 5A), leading to minimal detectable colonization after 7 dpi (Figure 5D). Furthermore, no *R. solanacearum* DNA was detected in plants treated with 2,4-DTBP alone or in the control group.

In conclusion, we investigated the effects of 2,4-DTBP on the growth and virulence of *R. solanacearum*. Our findings demonstrate that 2,4-DTBP significantly hindered growth, affecting its morphology, biofilm formation, and transcriptome. Furthermore, 2,4-DTBP inhibited membrane permeability and virulence. These mechanisms offer promising avenues for 2,4-DTBP-based interventions to control *R. solanacearum*. Additionally, these insights may shed light on the effects of similar *Ralstonia* species.

## AUTHOR INFORMATION

### Corresponding Author

**Peiqing Liu** – Fujian Key Laboratory for Monitoring and Integrated Management of Crop Pests, Institute of Plant Protection, Fujian Academy of Agricultural Sciences, Fuzhou 350003, China; Institute of Tobacco Science, Nanping Tobacco Company, Nanping 353000, China; [orcid.org/0000-0002-0997-363X](https://orcid.org/0000-0002-0997-363X); Email: [liupeiqing11@163.com](mailto:liupeiqing11@163.com)

### Authors

**Le Yang** – Fujian Key Laboratory for Monitoring and Integrated Management of Crop Pests, Institute of Plant Protection, Fujian Academy of Agricultural Sciences, Fuzhou 350003, China

**Rongbo Wang** – Fujian Key Laboratory for Monitoring and Integrated Management of Crop Pests, Institute of Plant Protection, Fujian Academy of Agricultural Sciences, Fuzhou 350003, China

**Wei Lin** – Institute of Tobacco Science, Nanping Tobacco Company, Nanping 353000, China

**Benjing Li** – Fujian Key Laboratory for Monitoring and Integrated Management of Crop Pests, Institute of Plant Protection, Fujian Academy of Agricultural Sciences, Fuzhou 350003, China

**Ting Jin** – Research and Development Center, Xiamen Canco Biotechnology Co., Ltd., Xiamen 361013, China

**Qiyong Weng** – Fujian Key Laboratory for Monitoring and Integrated Management of Crop Pests, Institute of Plant Protection, Fujian Academy of Agricultural Sciences, Fuzhou 350003, China

**Meixiang Zhang** – College of Life Sciences, Shaanxi Normal University, Xian 710119, China

Complete contact information is available at:

<https://pubs.acs.org/10.1021/acsomega.3c07887>

### Author Contributions

<sup>†</sup>L.Y. and R.W. contributed equally.

### Notes

The authors declare no competing financial interest.

## ACKNOWLEDGMENTS

The authors are grateful to the Natural Science Foundation of China [Grant Number 32072400], the Natural Science Foundation of Fujian Province [Grant Numbers 2021J01478, 2023R1072, and 2022J0143534], the Science and Technology Projects in Xiamen [Grant Number 3502Z20221018], the Project of Nanping Tobacco [Grant Number 2022350700240100], and the Project of FAAS [Grant Numbers GJYS202204, CXPT202105, XTCXGC2021017, and XTCXGC2021011].

## REFERENCES

- Hikichi, Y.; Takeshi, Y.; Shintaro, T.; Rena, S.; Kazuhiro, N.; Ayami, K.; Akinori, K.; Kouhei, O. Global regulation of pathogenicity mechanism of *Ralstonia solanacearum*. *Plant Tissue Cult. Lett.* **2007**, *24* (1), 149–154.
- Bereika, M. F. F.; Moharam, M. H.; Abo-Elyousr, K. A.; Asran, M. R. Investigation of virulence diversity in *Ralstonia solanacearum* isolates by a random amplified polymorphic DNA collected from Egyptian potato fields. *Arch. Phytopathol. Plant Prot.* **2022**, *55* (10), 1201–1218.
- Cai, L.; Chen, J.; Liu, Z.; Wang, H.; Yang, H.; Ding, W. Magnesium Oxide Nanoparticles: Effective Agricultural Antibacterial Agent Against *Ralstonia solanacearum*. *Front. Microbiol.* **2018**, *9*, 790.
- Hikichi, Y.; Yuka, M.; Shiho, I.; Kazusa, H.; Kouhei, O.; Akinori, K.; Kenji, K. Regulation Involved in Colonization of Intercellular Spaces of Host Plants in *Ralstonia solanacearum*. *Front. Plant Sci.* **2017**, *8*, 967.
- Gajewska, E.; Bernat, P.; Ugoński, J. D.; Odowska, M. Effect of Nickel on Membrane Integrity, Lipid Peroxidation and Fatty Acid Composition in Wheat Seedlings. *J. Agron. Crop Sci.* **2012**, *198* (4), 286–294.
- Mori, Y.; Inoue, K.; Ikeda, K.; Nakayashiki, H.; Higashimoto, C.; Ohnishi, K.; Kiba, A.; Hikichi, Y. The vascular plant-pathogenic bacterium *Ralstonia solanacearum* produces biofilms required for its virulence on the surfaces of tomato cells adjacent to intercellular spaces. *Mol. Plant Pathol.* **2016**, *17* (6), 890–902.
- Hayashi, K.; Wakana, S.; Kenji, K.; Akinori, K.; Kouhei, O. Major exopolysaccharide, EPS I, is associated with the feedback loop in the quorum sensing of *Ralstonia solanacearum* strain OE1–1. *Mol. Plant Pathol.* **2019**, *20* (12), 1740–1747.

- (8) Yuliar, Nion, Y. S.; Toyota, K. Recent Trends in Control Methods for Bacterial Wilt Diseases Caused by *Ralstonia solanacearum*. *Microbes Environ.* **2015**, *30* (1), 1–11.
- (9) Imada, K.; Sakai, S.; Kajihara, H.; Tanaka, S.; Ito, S. Magnesium oxide nanoparticles induce systemic resistance in tomato against bacterial wilt disease. *Plant Pathol.* **2016**, *65* (4), 551–560.
- (10) Wang, S.; Bai, Z.; Zhang, Z.; Bi, J.; Wang, E.; Sun, M.; Asante-Badu, B.; Zhang, J.; Njyenawe, M.; Song, A.; Fan, F. Organic or Inorganic Amendments Influence Microbial Community in Rhizosphere and Decreases the Incidence of Tomato Bacterial Wilt. *Agronomy* **2022**, *12* (12), 3029.
- (11) Zhu, H. H.; Yao, Q. Localized and Systemic Increase of Phenols in Tomato Roots Induced by *Glomus versiforme* Inhibits *Ralstonia solanacearum*. *J. Phytopathol.* **2004**, *152* (10), 537–542.
- (12) Xu, B.; Chang, S. Total Phenolics, Phenolic Acids, Isoflavones, and Anthocyanins and Antioxidant Properties of Yellow and Black Soybeans As Affected by Thermal Processing. *J. Agric. Food Chem.* **2008**, *56* (16), 7165–7175.
- (13) Viszwapriya, D.; Prithika, U.; Deebika, S.; Balamurugan, K.; Pandian, S. K. In vitro and in vivo antibiofilm potential of 2,4-Di-tert-butylphenol from seaweed surface associated bacterium *Bacillus subtilis* against group A streptococcus. *Microbiol. Res.* **2016**, *191*, 19–31.
- (14) Zhao, F.; Wang, P.; Lucardi, R. D.; Su, Z.; Li, S. Natural Sources and Bioactivities of 2,4-Di-Tert-Butylphenol and Its Analogs. *Toxins* **2020**, *12* (1), 35.
- (15) Doheny-Adams, T.; Lilley, C. J.; Barker, A.; Ellis, S.; Wade, R.; Atkinson, H. J.; Urwin, P. E.; Redeker, K.; Hartley, S. E. Constant isothiocyanate-release potentials across biofumigant seeding rates. *J. Agric. Food Chem.* **2018**, *66*, 5108–5116.
- (16) Dharni, S.; Gupta, S.; Maurya, A.; Samad, A.; Patra, D. D.; et al. Purification, characterization, and in vitro activity of 2,4-Di-tert-butylphenol from *Pseudomonas monteilii* PsF84: conformational and molecular docking studies. *J. Agric. Food Chem.* **2014**, *62* (26), 6138–6146.
- (17) Wang, Y. N.; Li, Y. B.; Huang, X. W.; Luo, L. X.; Cao, Y. S.; Li, J. Q. Antimicrobial activity of allyl isothiocyanate on common plant pathogens. *Chin. Sci. Pap.* **2018**, *13*, 692–697.
- (18) Pelyuntha, W.; Chaiyasut, C.; Kantachote, D.; Sirilun, S. Organic acids and 2,4-Di-tert-butylphenol: major compounds of *Weissella confusa* WM36 cell-free supernatant against growth, survival and virulence of *Salmonella* Typhi. *PeerJ* **2020**, *8* (5), No. e8410.
- (19) Yang, L.; Liu, X.; Zhuang, X.; Feng, X.; Zhong, L.; Ma, T. Antifungal Effects of Saponin Extract from Rhizomes of *Dioscorea panthaica* Prain et Burk against *Candida albicans*. *Evid-Based. Complement. Altern. Med.* **2018**, *2018*, No. 6095307.
- (20) Choi, S. J.; Kim, J. K.; Kim, H. K.; Harris, K.; Kim, C. J.; Park, G. G.; Park, C. S.; Shin, D. H. 2,4-Di-tert-butylphenol from sweet potato protects against oxidative stress in PC12 cells and in mice. *J. Med. Food* **2013**, *16* (11), 977–983.
- (21) Gutteridge, J. M. Lipid peroxidation and antioxidants as biomarkers of tissue damage. *Clin. Chem.* **1995**, *41*, 1819–1828.
- (22) Gajewska, E.; Bernat, P.; Ugoński, J. D.; Sk Odowska, M. Effect of Nickel on Membrane Integrity, Lipid Peroxidation and Fatty Acid Composition in Wheat Seedlings. *J. Agron. Crop Sci.* **2012**, *198* (4), 286–294.
- (23) Bai, S.; Wang, X.; Guo, M.; Cheng, G.; Khan, A.; Yao, W.; Gao, Y.; Li, J. Selection and evaluation of reference genes for quantitative real-time PCR in tomato (*Solanum lycopersicum* L.) inoculated with *Oidium neolycopersici*. *Agronomy* **2022**, *12*, 3171.
- (24) Cui, J.; Zhang, E.; Zhang, X.; Wang, Q.; Liu, Q. Effects of 2, 4-di-tert-butylphenol at different concentrations on soil functionality and microbial community structure in the Lanzhou lily rhizosphere. *Appl. Soil Ecol.* **2022**, *172*, No. 104367.
- (25) Seenivasan, A.; Manikkam, R.; Kaari, M.; Sahu, A.; Said, M.; Dastager, S. 2, 4-Di-tert-butylphenol (2, 4-DTBP) purified from *Streptomyces* sp. KCA1 from *Phyllanthus niruri*: Isolation, characterization, antibacterial and anticancer properties. *J. King Saud Univ. Sci.* **2022**, *34* (5), No. 102088.
- (26) Kushveer, J.; Sharma, R.; Samantaray, M.; Amutha, R.; Sarma, V. Purification and evaluation of 2, 4-di-tert butylphenol (DTBP) as a biocontrol agent against phyto-pathogenic fungi. *Fungal Biol.* **2023**, *127* (6), 1067–1074.
- (27) Jeon, D. H.; Young, A.; Park, K.; Lee, K.; Park, H. Antioxidants and their migration into food simulants on irradiated LLDPE film. *LWT – Food Sci. Technol.* **2007**, *40* (1), 151–156.
- (28) Halim, N. A.; Ma, N.; Sahid, I.; Chuah, T. Effects of 2,4-Di-tert-butylphenol and selected herbicides which induced lipid peroxidation on quantum yield and membrane integrity of weedy plants under dark and light conditions. *Sains Malays.* **2018**, *47*, 261–268.
- (29) Kaari, M.; Joseph, J.; Manikkam, R.; Kalyanasundaram, R.; Sivaraj, A.; Anbalmani, S.; Said, M.; Dastager, S.; Ramasamy, B.; et al. A novel finding: 2, 4-Di-tert-butylphenol from *Streptomyces bacillaris* ANS2 effective against *Mycobacterium tuberculosis* and cancer cell lines. *Appl. Biochem. Biotechnol.* **2023**, *195*, 6572–6585.
- (30) Ye, C.; Liu, Y. X.; Zhang, J. X.; Li, T. Y.; Zhang, Y. J.; Guo, C. W.; Yang, M.; He, X. H.; Zhu, Y. Y.; Huang, H. C.; Zhu, S. S.  $\alpha$ -Terpineol fumigation alleviates negative plant-soil feedbacks of *Panax notoginseng* via suppressing Ascomycota and enriching antagonistic bacteria. *Phytopathol. Res.* **2021**, *3*, 13.
- (31) Elexson, N.; Afsah-Hejri, L.; Rukayadi, Y.; Soopna, P.; Son, R.; et al. Effect of detergents as antibacterial agents on biofilm of antibiotics-resistant *Vibrio parahaemolyticus* isolates. *Food Control* **2014**, *35* (1), 378–385.
- (32) Irankhah, S.; Abdi Ali, A.; Reza Soudi, M.; Gharavi, S.; Ayati, B. Highly efficient phenol degradation in a batch moving bed biofilm reactor: benefiting from biofilm-enhancing bacteria. *World J. Microbiol. Biotechnol.* **2018**, *34*, 164.
- (33) McCall, I. C.; Betanzos, A.; Weber, D. A.; Nava, P.; Miller, G. W.; Parkos, C. A. Effects of phenol on barrier function of a human intestinal epithelial cell line correlate with altered tight junction protein localization. *Toxicol. Appl. Pharmacol.* **2009**, *241* (1), 61–70.
- (34) Jagani, S.; Chelikani, R.; Kim, D. S. Effects of phenol and natural phenolic compounds on biofilm formation by *Pseudomonas aeruginosa*. *Biofouling* **2009**, *25* (4), 321–324.
- (35) Aissou, N.; Mahjoubi, M.; Nas, F.; et al. Antibacterial Potential of 2,4-Di-tert-Butylphenol and Calixarene-Based Prodrugs from Thermophilic *Bacillus licheniformis* Isolated in Algerian Hot Spring. *Geomicrobiol. J.* **2019**, *36* (1), 53–62.
- (36) Liu, J. M.; Wang, S. S.; Zheng, X.; Jin, N.; Wang, F. Z.; et al. Antimicrobial Activity Against Phytopathogens and Inhibitory Activity on Solanine in Potatoes of the Endophytic Bacteria Isolated From Potato Tubers. *Front. Microbiol.* **2020**, *11*, No. 570926.
- (37) Ehlers, G. A.; Rose, P. D. Immobilized white-rot fungal biodegradation of phenol and chlorinated phenol in trickling packed-bed reactors by employing sequencing batch operation. *Bioresour. Technol.* **2005**, *96*, 1264–1275.
- (38) Ma, Y.; Li, L.; Awasthi, M. K.; Tian, H.; He, W.; et al. Time-course transcriptome analysis reveals the mechanisms of *Burkholderia* sp. adaptation to high phenol concentrations. *Appl. Microbiol. Biotechnol.* **2020**, *104*, 5873–5887.
- (39) Dias, M. C. Phytotoxicity: An Overview of the Physiological Responses of Plants Exposed to Fungicides. *J. Bot.* **2012**, *2012*, No. 135479.
- (40) Zhao, W. B.; Zhao, Z. M.; Ma, Y.; Li, A. P.; Zhang, Z. J.; Hu, Y. M.; Zhou, Y.; Wang, R.; Luo, X. F.; Zhang, B. Q.; et al. Antifungal activity and preliminary mechanism of pristimerin against *Sclerotinia sclerotiorum*. *Ind. Crops Prod.* **2022**, *185*, No. 115124.
- (41) Sinha, B. A.; Smejtek, P. Effect of 3-phenylindole on lipophilic ion and carrier-mediated ion transport across bilayer lipid membranes. *J. Membr. Biol.* **1983**, *71*, 119–130.
- (42) Shen, Q.; Wei, Z.; Hongbo, L.; Liangbin, H.; Haizhen, M. ROS Involves the Fungicidal Actions of Thymol against Spores of *Aspergillus flavus* via the Induction of Nitric Oxide. *PLoS One* **2016**, *11* (5), No. e0155647.
- (43) Yue, Y.; Wang, Z.; Zhong, T.; Guo, M.; Huang, L.; Yang, L.; Kan, J.; Zalán, Z.; Hegyi, F.; Takács, K. Antifungal mechanisms of volatile organic compounds produced by *Pseudomonas fluorescens*

ZX as biological fumigants against *Botrytis cinerea*. *Microbiol. Res.* **2023**, *267*, No. 127253.

(44) Jambunathan, N. Determination and Detection of Reactive Oxygen Species (ROS), Lipid Peroxidation, and Electrolyte Leakage in Plants. *Methods Mol. Biol.* **2010**, *639*, 292–298.

(45) Steel, C. C.; Drysdale, R. B. Electrolyte leakage from plant and fungal tissues and disruption of liposome membranes by  $\alpha$ -tomatine. *Phytochemistry* **1988**, *27* (4), 1025–1030.

(46) Zhang, M.; Ge, J.; Yu, X. Transcriptome Analysis Reveals the Mechanism of Fungicidal of Thymol Against *Fusarium oxysporum* f. sp. *niveum*. *Curr. Microbiol.* **2018**, *75*, 410–419.

(47) Zhao, M.; Ge, Y.; Xu, Z.; Ouyang, X.; Jia, Y.; Liu, J.; Zhang, M.; An, Y. A BTB/POZ domain-containing protein negatively regulates plant immunity in *Nicotiana benthamiana*. *Biochem. Biophys. Res. Commun.* **2022**, *600*, 54–59.

(48) Nakano, M.; Mukaihara, T. The type III effector RipB from *Ralstonia solanacearum* RS1000 acts as a major avirulence factor in *Nicotiana benthamiana* and other *Nicotiana* species. *Mol. Plant Pathol.* **2019**, *20* (9), 1237–1251.

(49) Li, Q.; Ai, G.; Shen, D.; Zou, F.; Wang, J.; Bai, T.; Chen, Y.; Li, S.; Zhang, M.; Jing, M.; Dou, D. A *Phytophthora capsici* Effector Targets ACD11 Binding Partners that Regulate ROS-Mediated Defense Response in *Arabidopsis*. *Mol. Plant* **2019**, *12* (4), 565–581.

(50) Mena, E.; Stewart, S.; Montesano, M.; de León, I. P. Soybean Stem Canker Caused by *Diaporthe caulivora*; Pathogen Diversity, Colonization Process, and Plant Defense Activation. *Front. Plant Sci.* **2020**, *10*, 1733.

(51) Landry, D.; González, M.; Deslandes, L.; Peeters, N. The large, diverse, and robust arsenal of *Ralstonia solanacearum* type III effectors and their in planta functions. *Mol. Plant Pathol.* **2020**, *21*, 1377–1388.